Extremely strong solvent dependence of the $S_1 \rightarrow S_0$ internal conversion lifetime of 12′-apo-β-caroten-12′-al

Duncan A. Wild,[a] Kathrin Winkler,[a] Sebastian Stalke,[a] Kawon Oum[b] and Thomas Lenzer*[ab]

Received 3rd February 2006, Accepted 6th April 2006
First published as an Advance Article on the web 26th May 2006
DOI: 10.1039/b601669c

The ultrafast internal conversion (IC) dynamics of the carbonyl carotenoid 12′-apo-β-caroten-12′-al has been investigated in solvents of varying polarity using time-resolved femtosecond transient absorption spectroscopy. The molecules were excited to the S_2 state by a pump beam of either 390 or 470 nm. The subsequent intramolecular dynamics were detected at several probe wavelengths covering the $S_0 \rightarrow S_2$ and $S_1 \rightarrow S_n$ bands. For the $S_1 \rightarrow S_0$ internal conversion process, a remarkably strong acceleration with increasing polarity was found, *e.g.*, lifetimes of $\tau_1 = 220$ ps (*n*-hexane), 91 ps (tetrahydrofuran) and 8.0 ps (methanol) after excitation at 390 nm. The observation can be rationalized by the formation of a combined S_1/ICT (intramolecular charge transfer) state in the more polar solvents. The effect is even stronger than the strongest one reported so far in the literature for peridinin. Addition of lithium salts to a solution of 12′-apo-β-caroten-12′-al in ethanol leads only to small changes of the IC time constant τ_1. In addition, we estimate an upper limit for the time constant τ_2 of the $S_2 \rightarrow S_1$ internal conversion process of 300 fs in all solvents.

1. Introduction

Carotenoids play a key role in photosynthesis, where they are involved in the light-harvesting process in the blue–green spectral region.[1] They also protect against excessive light by quenching both singlet and triplet states of bacteriochlorophylls.[2] An important sub-class are carotenoids containing carbonyl groups, which may or may not be incorporated into the conjugated carbon chain. For instance, fucoxanthin is the carotenoid with the highest abundance worldwide, representing about 60% of the carotenoids produced by marine algae. Peridinin is found in large amounts in oceanic dinoflagellates,[3–6] and is the main light-harvesting pigment in the peridinin–chlorophyll-a protein (PCP) complex.[7] To understand the photophysics and energy transfer pathways in such complex systems it is necessary as a first step to understand the dynamics of the isolated carotenoid species and other structurally related carbonyl carotenoids in simple environments such as solvents of different polarity.

In the simplest model, the photophysics of carotenoids can be described by three electronic states. The one-photon transition from the electronic ground state S_0 ($1A_g^-$) to the first excited singlet state S_1 ($2A_g^-$) is symmetry forbidden (labels are based on idealized C_{2h} polyene symmetry). The strong absorption in the visible region of the spectrum is due to the transition to the second electronically excited singlet state S_2 ($1B_u^+$). The dynamics after photoexcitation are governed by ultrafast internal conversion (IC) processes, where typical lifetimes τ_2 for the $S_2 \rightarrow S_1$ transition are <200 fs. In contrast, the $S_1 \rightarrow S_0$ IC is usually much slower, with relaxation time constants τ_1 on the order of picoseconds to nanoseconds, depending on the structure and conjugation length of the carotenoid.[1]

Carbonyl carotenoids show strong variations of the solvent dependence of τ_1. As an example, for the C_{40} carotenoid astaxanthin with two keto groups located on its terminal β-ionone rings, τ_1 is virtually solvent independent with a value of about 5 ps, as shown in very recent ultrafast transient absorption (TA) and transient lens (TL) pump–probe experiments.[8,9] In marked contrast, the lifetime of peridinin in its S_1 state in nonpolar solvents is roughly 160 ps, whereas in polar environments it decreases to about 10 ps.[6,10,11] The large change in the S_1 lifetime of peridinin was thought to be unique among carotenoids and related to its specific structure, where a carbonyl group is located in the middle of the conjugated chain attached *via* a lactone ring.[10] Its specific nonradiative dynamics were explained by the presence of a combined S_1/ICT (intramolecular charge transfer) state. For this state, polar solvents probably stabilize a structure where a substantial shift of electron density from the polyene chain to the C═O group can occur.[11,12] This was underlined by time-resolved spectroscopic investigations which found excited state absorption (ESA) bands in the 600–700 nm region and stimulated emission (SE) features around 950 nm. The intensity of these bands increased with the degree of CT character.[11]

The structural prerequisites for a carotenoid to show a strong variation of τ_1 with solvent polarity are not yet clear,

[a] *Max-Planck-Institut für biophysikalische Chemie, Abt. Spektroskopie und Photochemische Kinetik (10100), Am Fassberg 11, D-37077 Göttingen, Germany. Fax: +49 551 201 1501; Tel: +49 551 201 1344*
[b] *Institut für Physikalische Chemie, Universität Göttingen, Tammannstrasse 6, D-37077 Göttingen, Germany. E-mail: tlenzer@gwdg.de; koum@gwdg.de; Fax: +49 551 39 3150; Tel: +49 551 39 12598*

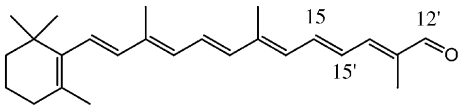

Fig. 1 Structure of 12′-apo-β-caroten-12′-al (conjugation 6O1β1).

and further systematic studies of other carbonyl containing carotenoids are clearly needed to understand the observed effects.[1,9,13] This study is intended as another step in this direction. We investigate for the first time 12′-apo-β-caroten-12′-al, a simple apocarotenoid having a terminal aldehyde group in conjugation with the rest of its carbon backbone (see Fig. 1). As in our earlier ultrafast spectroscopic studies we apply the convenient nomenclature of Polívka and Sundström.[1,9,13] The conjugated system of the carotenoid is described by the abbreviation *NOkβj*, where *N* is the number of conjugated C=C bonds in the carotenoid backbone. O*k* indicates that the conjugation is extended to *k* carbonyl groups, and β*j* describes the fact that the conjugation is extended to *j* C=C bonds located at a terminal β-ionone ring. The conjugated system of 12′-apo-β-caroten-12′-al is thus characterized as "6O1β1". As we will demonstrate, 12′-apo-β-caroten-12′-al shows an even stronger solvent dependence of the IC time constant τ_1 than peridinin. It is also far stronger than that observed for two other apocarotenal species studied previously.[14]

2. Experimental setup

The output of a Ti:sapphire oscillator-regenerative amplifier system (780 nm, 1 kHz, 1 mJ pulse^{-1}) was split up into two beams. One half of the energy was frequency-doubled to 390 nm in a BBO crystal and used directly as a pump beam to excite 12′-apo-β-caroten-12′-al into higher vibrational levels of the S_2 state. The other half was either frequency doubled to 390 nm in a BBO crystal and used directly for detection of the absorption recovery in the electronic ground state *via* the $S_0 \rightarrow S_2$ absorption band or sent to a home-built blue-pumped two-stage noncollinearly phase-matched optical parametric amplifier (NOPA).[15–17] Its output was subsequently compressed by a pair of quartz prisms. The NOPA was tuned to two probe wavelengths, 575 and 630 nm, to detect the dynamics of the transient S_1 population *via* the $S_1 \rightarrow S_n$ absorption. In some of the experiments the NOPA was tuned to 470 nm and used as a pump to excite ground state molecules to lower vibrational levels in the S_2 state. The dynamics were then probed at 390 nm using the frequency-doubled Ti:sapphire laser output. The pump and probe pulses were time-delayed with respect to each other by means of a computer-controlled delay stage. They were then attenuated and weakly focused into the sample cell under a small angle. The diameter of the light spot on the sample was approximately 250 μm. The relative polarizations of the pump and probe beams were adjusted to 54.7° (magic angle) to avoid any contributions from orientational relaxation effects. Probe energies were measured by photodiodes in front of and behind the flow quartz cuvette (1 mm path length), which contained the carotenoid solution. A chopper wheel blocked every second pump pulse in order to independently measure possible drifts of the background absorption. The change in optical density (ΔOD) was then determined as:

$$\Delta OD = OD_{exc} - OD_0 = \ln(I/I_0)_0 - \ln(I/I_0)_{exc} \qquad (1)$$

where OD_{exc} and OD_0 are the optical densities with and without the pump beam, respectively. $(I/I_0)_{exc}$ and $(I/I_0)_0$ are the ratios of the light intensities behind and in front of the cuvette with and without the pump beam. Typically, 1000 laser shots were averaged for each point in each pass of the time range investigated. The time range was then scanned four times to produce a single spectrum, and at least four spectra were averaged to give the final result. The time resolution of the setup was typically between 100 and 150 fs. Typical energies for the pump and probe beams were 2 μJ pulse^{-1} or less. We observed no sample degradation, as shown by comparison of absorption spectra of the carotenoid solution before and after the measurements. No dependence of the signals on the carotenoid concentration was found, which was typically between 2.5 and 7.5 × 10^{-5} M. Small coherence artefacts were found for some of the solvents within the cross-correlation of our pump and probe pulses. They have no influence on the time constants τ_1 reported below. Highly purified *all-trans* (*all-E*) 12′-apo-β-caroten-12′-al samples were generously provided by BASF AG with a purity >97%. All solvents had a purity ≥ 99%. Absorption spectra of 12′-apo-β-caroten-12′-al were recorded using a Varian Cary 5E spectrometer.

3. Results and discussion

3.1 Ground state absorption spectra of 12′-apo-β-caroten-12′-al in different solvents

$S_0 \rightarrow S_2$ steady-state absorption spectra of 12′-apo-β-caroten-12′-al in all solvents can be found in Fig. 2. Table 1 gives an overview of the corresponding absorption maxima λ_{max}. The solvent dependence of the spectra is in line with earlier observations made for structurally similar carotenoids.[1,14] In

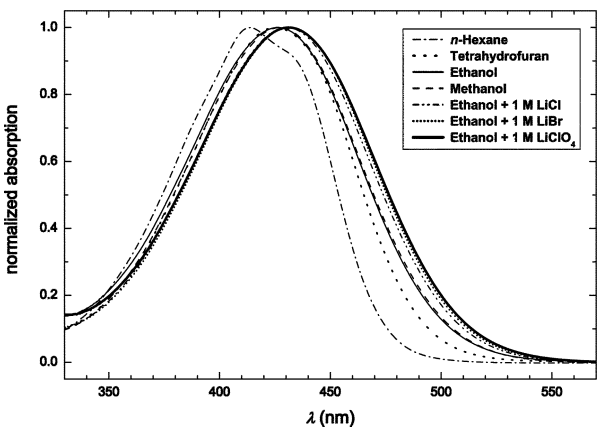

Fig. 2 $S_0 \rightarrow S_2$ steady-state absorption spectra of 12′-apo-β-caroten-12′-al in solvents of different polarity. Dash–dotted line: *n*-hexane, dotted line: tetrahydrofuran, thin solid line: ethanol, dashed line: methanol, dash–dot–dotted line: ethanol + 1 M LiCl, short dotted line: ethanol + 1 M LiBr, thick solid line: ethanol + 1 M $LiClO_4$.

Table 1 Lifetime $\tau_1(S_1 \rightarrow S_0)$ of 12′-apo-β-caroten-12′-al in various solvents. TA pump wavelengths: 390 nm and 470 nm, probe wavelengths: 470, 575 and 630 nm. λ_{max} values correspond to the position of the maximum of the $S_0 \rightarrow S_2$ steady-state absorption spectrum in each solvent (Fig. 1). Only upper limits can be given for the time constant of the IC process $S_2 \rightarrow S_1$, where one typically finds $\tau_2(S_2 \rightarrow S_1) \leq 300$ fs

		τ_1/ps			
		Pump 470 nm	Pump 390 nm		
Solvent	λ_{max}/nm	Probe 390 nm	Probe 390 nm	Probe 575 nm	Probe 630 nm
n-Hexane	414	205	224	221	217
Tetrahydrofuran	425	96	92	95	85
Ethanol	426	18.6	22.6	22.2	18.5
Ethanol/ 1 M LiCl	430	—	—	24.1	—
Ethanol/ 1 M LiBr	431	—	—	23.0	—
Ethanol/ 1 M $LiClO_4$	431	—	—	19.1	—
Methanol	427	6.7	8.0	8.2	7.9

the nonpolar solvent, *n*-hexane, three peaks appear as very weak shoulders which are assigned to a vibrational progression resulting from the combination of two symmetric vibrational C–C and C=C stretching modes. In polar solvents the vibrational structure disappears completely and one finds an asymmetric broadening of the band toward longer wavelengths. It has been suggested that this effect is most likely due to the dipolar character of the electronic ground state S_0, where stabilization of a negative charge on the carbonyl oxygen in polar solvents leads to the presence of a broader distribution of conformers. The latter results in a loss of vibrational structure and an additional broadening of the spectra, and possibly an increased mixing of the S_2 state with other excited electronic states.[6,12,18] In addition, we investigated the changes in the spectral shift of 12′-apo-β-caroten-12′-al when an ionic solution is created by adding salts like $LiClO_4$, LiBr and LiCl to an organic solvent, here ethanol. For all lithium salts we observed a pronounced additional red shift and a slightly asymmetric broadening (Fig. 2). The red shifts are similar for all salts. There is only a slight systematic increase of the red shift with the size of the anion. These findings are in agreement with earlier studies by the groups of Maroncelli and Huppert of coumarin dyes in different ionic solvents.[19,20] The effect can be rationalized by a simple model assuming a substantial fraction of the solute molecules to have a Li^+ ion situated close to a negative partial charge, *e.g.*, the oxygen atom of the carbonyl group of the carotenoid. This would be a favorable site for cation binding, and as the carotenoid experiences a more polar surrounding, one observes an additional bathochromic shift compared to the pure solvent.[19,20]

3.2 Probe wavelength dependence of transient absorption signals

Experimental TA signals for 12′-apo-β-caroten-12′-al in *n*-hexane and methanol can be found in Fig. 3 and 4, where we show ΔOD [eqn (1)] as a function of the delay time between

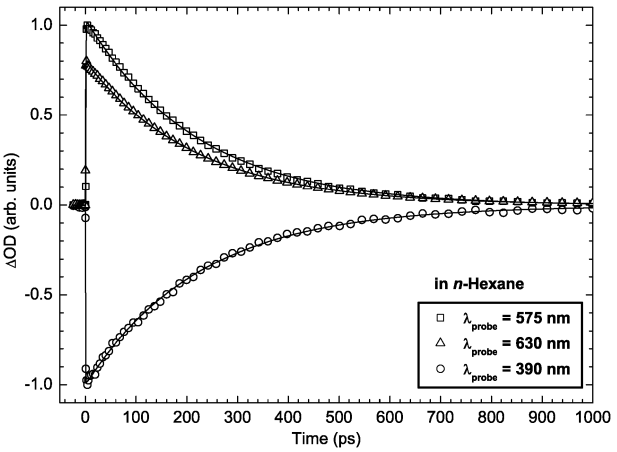

Fig. 3 TA signals of 12′-apo-β-caroten-12′-al in *n*-hexane after excitation to the S_2 state at 390 nm. □ and △: $S_1 \rightarrow S_n$ absorption at 575 and 630 nm, respectively, from the first electronically excited state, which is populated and depleted in the course of the intramolecular relaxation. ○: $S_0 \rightarrow S_2$ absorption at 390 nm. Solid lines are fits from the kinetic model, see the text. Time constants τ_1 for the $S_1 \rightarrow S_0$ IC process can be found in Table 1.

the pump and probe pulses. The carotenoid was pumped to the S_2 state at 390 nm, and the subsequent dynamics were probed at the wavelengths 390, 575, and 630 nm. The signals at the probe wavelength of 390 nm show an immediate drop at $t = 0$. Subsequently, the negative signal decays back to zero on a much slower timescale. The fast initial drop is due to up-pumping of 12′-apo-β-caroten-12′-al to the S_2 state. After an initial very fast IC step $S_2 \rightarrow S_1$, which typically occurs with a time constant $\tau_2 < 200$ fs for most carotenoids,[1] the second IC step $S_1 \rightarrow S_0$ takes place resulting in a much slower final recovery of the absorption signal. From analysis on the basis of a kinetic model (see below) we determine τ_1 to be 224 ps in *n*-hexane and 8.0 ps in methanol.

The other probe wavelengths 575 and 630 nm are located in a region where the excited state absorption band $S_1 \rightarrow S_n$ (or S_1/ICT) of carbonyl carotenoids is expected.[11] The fast initial rise of the signal within our time resolution is therefore due to

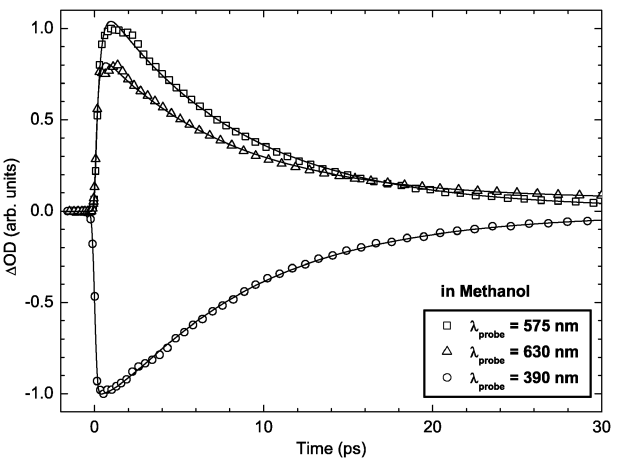

Fig. 4 Same as in Fig. 3 but in methanol.

preparation of the S_1 state population by excitation of the molecules to the S_2 state and the subsequent IC process $S_2 \rightarrow S_1$. We can only give a rough estimate for this IC step of $\tau_2 \leq 300$ fs. In *n*-hexane the excited state absorption profiles decay with the time constants $\tau_1(S_1 \rightarrow S_0) = 221$ and 217 ps, respectively, well within the error bars of the value from the population recovery in S_0 probed at 390 nm. The corresponding time constants for methanol are 8.2 and 7.9 ps. In all the solvents we see a decrease of τ_1 at the probe wavelength 630 nm. It could be that S_1 vibrational relaxation, *i.e.* vibrational cooling of the solute by collisions with solvent molecules, results in a narrowing of the ESA band, which could be more pronounced on the red band edge.[21,22]

While after excitation at 390 nm all TA signals in *n*-hexane decay to zero, this is not the case in the solvents tetrahydrofuran and methanol. The signal does not fully recover, and the residual bleach is typically on the order of 1–3%. In a similar way, the excited state absorption signals at 575 and 630 nm do not decay completely, and show a small residual signal in these solvents (Fig. 4). The effect is not due to solvent absorption, which was confirmed by additional transient absorption measurements in the pure solvents. The small offset varied slightly with pump energy, but leveled off below pulse energies of 1 μJ. One tentative explanation would be that a very small fraction of the population remains trapped in a long-lived state, possibly a triplet, which is known to absorb above 500 nm for carotenoids like zeaxanthin.[23] It is, however, unclear at the present stage how and why such a state would be formed in more polar solvents only. Clearly additional time-resolved measurements at various probe wavelengths should help with addressing this issue and are currently underway.

3.3 Kinetic scheme and fitting functions

To fit the TA signals at the different probe wavelengths, kinetic equations for a simple scheme of two consecutive IC processes $S_2 \rightarrow S_1 \rightarrow S_0$ after preparation of the S_2 population by a Gaussian pump laser pulse with the width γ_1 were set up:

$$\frac{d[S_2]}{dt} = k \exp\left(-\frac{t^2}{\gamma_1^2}\right) - k_2[S_2] \quad (2)$$

$$\frac{d[S_1]}{dt} = k_2[S_2] - k_1[S_1] \quad (3)$$

$$\frac{d[S_0]}{dt} = -k \exp\left(-\frac{t^2}{\gamma_1^2}\right) + k_1[S_1] \quad (4)$$

Here $[S_2]$, $[S_1]$ and $[S_0]$ are the concentrations of 12′-apo-β-caroten-12′-al molecules in the S_2, S_1 and S_0 states, respectively. k is a prefactor characterizing the amount of S_2 population initially prepared by the pump pulse. k_2 and k_1 are the rate constants for the IC processes $S_2 \rightarrow S_1$ and $S_1 \rightarrow S_0$, respectively, which are converted to the corresponding time constants *via* $\tau_2 = 1/k_2$ and $\tau_1 = 1/k_1$. The system can then be fully solved analytically, and the resulting expressions are convoluted with the probe pulse assuming a Gaussian time dependence of the intensity characterized by the width γ_2. In this way, the finite width of the probe laser pulse is taken into account, leading to the following final expressions:

$$[S_2] = \frac{k\gamma_1\sqrt{\pi}}{2} e^{-k_2 t + \frac{k_2^2(\gamma_1^2+\gamma_2^2)}{4}} \left(1 + \mathrm{erf}\left[\frac{2t - k_2(\gamma_1^2+\gamma_2^2)}{2\sqrt{\gamma_1^2+\gamma_2^2}}\right]\right) \quad (5)$$

$$[S_1] = \frac{k_2 k\gamma_1\sqrt{\pi}}{2(k_2-k_1)} \left(\begin{array}{l} e^{\frac{\gamma_1^2+\gamma_2^2}{4}k_1^2 - k_1 t}\left(1 + \mathrm{erf}\left[\frac{2t - k_1(\gamma_1^2+\gamma_2^2)}{2\sqrt{\gamma_1^2+\gamma_2^2}}\right]\right) \\ -e^{\frac{\gamma_1^2+\gamma_2^2}{4}k_2^2 - k_2 t}\left(1 + \mathrm{erf}\left[\frac{2t - k_2(\gamma_1^2+\gamma_2^2)}{2\sqrt{\gamma_1^2+\gamma_2^2}}\right]\right) \end{array} \right) \quad (6)$$

$$[S_0] = \frac{k\gamma_1\sqrt{\pi}}{2(k_1-k_2)} \left(\begin{array}{l} k_2 e^{\frac{\gamma_1^2+\gamma_2^2}{4}k_1^2 - k_1 t}\left(1 + \mathrm{erf}\left[\frac{2t - k_1(\gamma_1^2+\gamma_2^2)}{2\sqrt{\gamma_1^2+\gamma_2^2}}\right]\right) \\ -k_1 e^{\frac{\gamma_1^2+\gamma_2^2}{4}k_2^2 - k_2 t}\left(1 + \mathrm{erf}\left[\frac{2t - k_2(\gamma_1^2+\gamma_2^2)}{2\sqrt{\gamma_1^2+\gamma_2^2}}\right]\right) \end{array} \right) \quad (7)$$

eqn (6) and (7) were used for fitting the measured absorption profiles using a Levenberg–Marquardt χ^2 minimization procedure[24] to obtain the fit lines in Fig. 3 and 4 and those given in the following sections. To model the small offset mentioned earlier, we added a separate jump function, which was assumed to rise to its final value within the time resolution of our setup. From the χ^2 analysis we estimate the uncertainties of the time constants τ_1 to be smaller than ten percent.

Note, that the simple model we apply here can very likely not account for fine details of the expected dynamics, as it does not include processes like vibrational relaxation or, *e.g.*, S_1/ICT stabilization.[11] Neglecting these steps is, however, not crucial to get sufficiently precise time constants τ_1.

3.4 Dependence of the transient absorption signals on the pump wavelength

In addition to the experiments with 390 nm pump wavelength, we carried out measurements at 470 nm, on the red edge of the $S_0 \rightarrow S_2$ absorption band. In this case, the 12′-apo-β-caroten-12′-al was excited near the 0–0 transition of the S_2 state, *i.e.*, with much less vibrational energy than for excitation at 390 nm. The nonradiative dynamics were then probed at 390 nm. An example with methanol as solvent is shown in Fig. 5. At the pump wavelength 470 nm we find a slightly smaller time constant for the $S_1 \rightarrow S_0$ IC than for 390 nm excitation for most of the solvents (see Table 1). It could be that excitation on the red edge at 470 nm preferentially excites different S_0 conformers.[12] These might show a different relaxation behavior after excitation. The very small absorption pedestal at long times is still present, however, again the uncertainty introduced for the fit of the time constant τ_1 is very small. Our data shows that the excess energy dependence of τ_1 is not dramatic. This is in line with a previous detailed study performed by Polívka and co-workers on the carotenoid zeaxanthin.[23] In fact, the minor changes in the lifetimes τ_1 with excitation wavelength in the solvent methanol is also in accord with the excitation wavelength dependence of peridinin in hydrogen-bonding solvents such as methanol.[12]

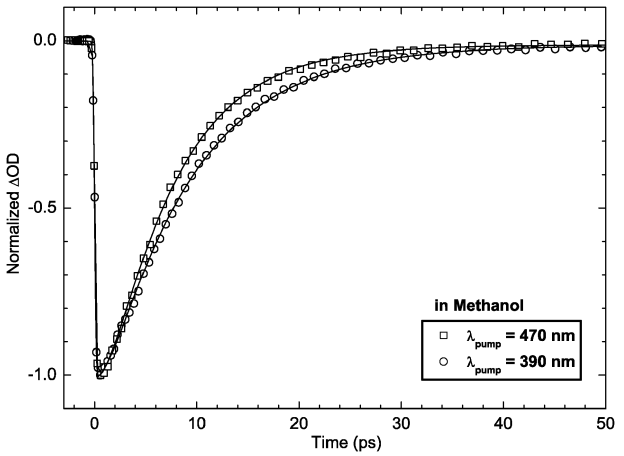

Fig. 5 Normalized TA signals of 12′-apo-β-caroten-12′-al in methanol after excitation to the S_2 state at different pump wavelengths. □: λ_{pump} = 470 nm, ○: λ_{pump} = 390 nm. Probe wavelength in both cases: 390 nm. Time constants τ_1 for the $S_1 \rightarrow S_0$ IC process can be found in Table 1.

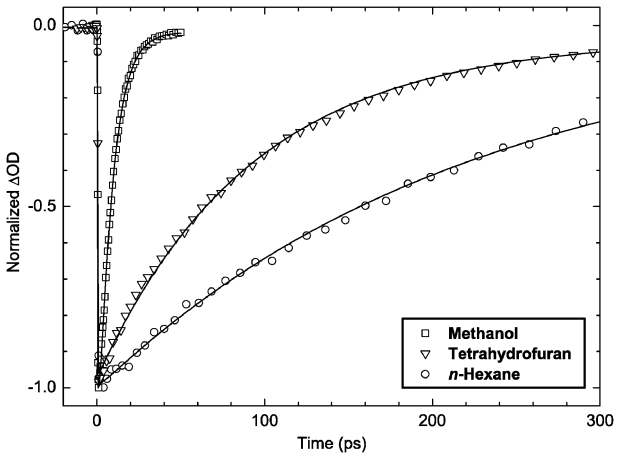

Fig. 6 Normalized TA signals of 12′-apo-β-caroten-12′-al in solvents of different polarity after excitation to the S_2 state at 390 nm. The dynamics is probed at 390 nm. □: in methanol, ▽: in THF, ○: in *n*-hexane. Time constants τ_1 for the $S_1 \rightarrow S_0$ IC process can be found in Table 1.

3.5 Solvent dependence of the IC time constant τ_1

A list of lifetimes $\tau_1(S_1 \rightarrow S_0)$ for 12′-apo-β-caroten-12′-al in different solvents can be found in Table 1. The solvents are arranged from top to bottom according to their polarity.[9,25–28] A comparison of transient absorption signals for the solvents *n*-hexane (nonpolar), tetrahydrofuran (THF, medium polarity) and methanol (high polarity) is shown in Fig. 6, including fits using the kinetic model [—, eqn (7)]. Most interestingly, we find an extremely strong solvent dependence on going from the nonpolar solvent *n*-hexane, to THF and methanol (τ_1 = 220, 91, and 8.0 ps, respectively, the averages of values for three probe wavelengths for pumping at 390 nm). In fact, the observed change by about a factor of 30(!) is even more pronounced than the strongest solvent dependence reported so far for the carbonyl carotenoid peridinin (see Table 2). The large change in the S_1 lifetime of peridinin was related to its specific structure, where an allene moiety and C═O function on the lactone ring extend the conjugated π-electron system of the carbon backbone.[10] Our experiments show that a C═O substituted apocarotenoid with a very simple structure has an even more drastic solvent effect.

A marked decrease of τ_1 in carbonyl carotenoids is typically explained by the appearance of considerable charge transfer character through formation of a combined "S_1/ICT" state in polar media.[1,11,12,14] In nonpolar solvents, the stepwise relaxation would then be $S_2 \rightarrow S_1 \rightarrow S_0$, whereas in polar solvents it can be described as $S_2 \rightarrow$ "S_1/ICT" $\rightarrow S_0$. A typical manifestation of the ICT character should be the formation of a stimulated emission band in the near infrared.[29] Preliminary TA measurements by us employing probe wavelengths of 780 and 800 nm indeed show evidence for such stimulated emission in polar solvents. This will be dealt with in more detail in a separate publication.[30]

Note that as a finer detail we see some variation of the time constant τ_1 with probe wavelength, especially some decrease at 630 nm (Table 1). It might be that the kinetic model we apply is too simple to account for all details of the dynamics, and that additional processes like S_1/ICT stabilization or vibrational relaxation are responsible for this effect. In future studies we therefore plan to extend the range of wavelengths, especially in the NIR region to find out if a S_1/ICT stabilization step is present as in the case of peridinin,[11] and analyze the data by a more complex model.

It is surprising that the S_1/ICT lifetimes for different C═O substituted apocarotenoids are nearly identical in polar solvents despite very different conjugation lengths. An example is shown in Table 2, where the τ_1 values of the three closely related aldehydes 12′-apo-β-caroten-12′-al (6O1β1), 8′-apo-β-caroten-8′-al (8O1β1) and 6′-apo-β-caroten-6′-al (9O1β1) are compared.[6,10,14,29,30] The 8′- and 6′-species differ from the 12′-apocarotenoid by addition of 2 or 3 additional conjugated C═C double bonds, respectively, however, interestingly all τ_1 values in methanol are almost identical, with values between 6 and 8 ps. In contrast, the strong decrease of the S_1 lifetime in *n*-hexane with increasing conjugation length is in very good agreement with that predicted by an energy-gap law approach.[10,31–33] Extension of the conjugated system apparently provides enough stabilization of the S_1 state even in nonpolar solvents. Theoretical studies are currently underway in our group to explain these effects.

Table 2 Comparison of the lifetimes $\tau_1(S_1 \rightarrow S_0)$ in nonpolar and polar solvents for 12′-apo-β-caroten-12′-al with those for 8′-apo-β-caroten-8′-al, 6′-apo-β-caroten-6′-al and peridinin

Carbonyl substituted carotenoid	Conjugation	τ_1/ps (*n*-hexane)	τ_1/ps (methanol)	Ref.
6′-apo-β-caroten-6′-al	9O1β1	12.0	6.3	14
8′-apo-β-caroten-8′-al	8O1β1	21.3	8.4	30
12′-apo-β-caroten-12′-al	6O1β1	220[a]	8.0[a]	This work
Peridinin	7LOA[b]	161	12	6, 10
		156	10.5	29

[a] Arithmetic averages of the values for the pump wavelength 390 nm in Table 1. [b] Nomenclature see ref. 1.

We have also investigated changes of the time constant τ_1 in 12′-apo-β-caroten-12′-al when salts are added to an ethanol solution. One would expect some changes in the polarity of the environment which might influence τ_1. To study this salt effect we used the three lithium salts LiCl, LiBr and $LiClO_4$. In each case 1 M salt was added to a solution of the carotenoid in ethanol. A comparison of the excited state absorption signals of 12′-apo-β-caroten-12′-al at the probe wavelength 575 nm in ethanol and in 1 M solutions of LiCl, LiBr and $LiClO_4$ in ethanol is shown in Fig. 7. Fits using our simple kinetic model provide time constants τ_1 of 22.2, 24.1, 23.0 and 19.1 ps (Table 1). In general the observed effect of the salt on the intramolecular dynamics is small. The results for LiCl and LiBr are very similar to the one in pure ethanol, and $LiClO_4$ shows a reduction of τ_1. The latter one could be tentatively interpreted as follows: The S_1/ICT state is likely characterized by a structure, where to some extent electron density is transferred from the polyene chain to the C═O group, written in a simplified way as R–C═O → R^+–C–O^-. In the $LiClO_4$ solution, arrangements might be favored, where the small Li^+ cation resides closer to the electronegative oxygen of the carbonyl group, and the perchlorate anion stabilizes the positive countercharge on the conjugated system. This could lead to an increased stabilization of the more polar S_1/ICT state relative to the S_0 state. Simple arguments on the basis of an energy gap law approach would then predict an increase of the nonradiative rate constant k_1 corresponding to a reduction of τ_1.[31–33] Indeed, this would be in agreement with the explanation of the stronger ICT character of the S_1/ICT state of peridinin in hydrogen-bonding solvents.[12] At the current point, however, it remains unclear why the other lithium salts behave differently. One could speculate that the absorption traces are influenced by different translational dynamics of the different ions, however, this sort of dynamics is expected to happen on longer timescales.[19,20] Clearly, measurements employing additional probe wavelengths, salts with different cations and systematic variation of the salt concentration are required to fully understand the observed effects. In addition, quantum mechanical modeling is definitely needed to confirm the simple picture outlined above.

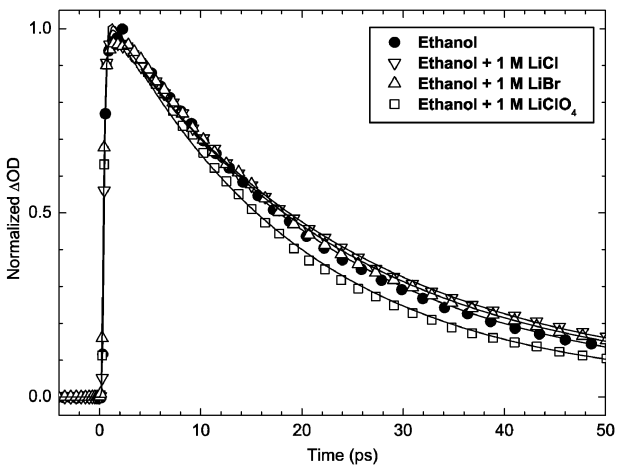

Fig. 7 Comparison of TA signals for 12′-apo-β-caroten-12′-al in ethanol with and without 1 M lithium salts. Pump wavelength: 390 nm, probe wavelength: 575 nm ($S_1 \rightarrow S_n$ absorption). ●: pure ethanol, ▽: ethanol + 1 M LiCl, △: ethanol + 1 M LiBr, □: ethanol + 1 M $LiClO_4$. Static absorption spectra of the solutions can be found in Fig. 2. For time constants see Table 1.

4. Conclusions

We have reported the first time-resolved transient absorption study of internal conversion processes in the apocarotenoid 12′-apo-β-caroten-12′-al. The carotenoid was generated with low and high vibrational excess energy in the S_2 state. The first internal conversion step to the S_1 state is extremely fast, and only an upper limit of 300 fs can be given for the time constant τ_2. For the subsequent step, the $S_1 \rightarrow S_0$ internal conversion, a remarkably strong acceleration with increasing solvent polarity has been found, with time constants τ_1 ranging from 220 ps in *n*-hexane to 8.0 ps in methanol. The observations can be rationalized by the stabilization of a combined S_1/ICT state in the more polar solvents, similar to the well-known case of peridinin. Addition of lithium salts results only in small changes of the time constant τ_1.

We are currently performing additional measurements at other wavelengths. Preliminary results at the probe wavelengths 780 nm and 800 nm show pronounced stimulated emission features in methanol and acetonitrile, which are a clear signature of the S_1/ICT state. Stimulated emission is, however, not observed in *n*-hexane. We are also carrying out complementary theoretical studies to understand the observed strong solvent dependence of τ_1 in more detail.

Acknowledgements

Financial support of this project by the Alexander von Humboldt Foundation within the "Sofja Kovalevskaja Program" in the framework of the future investment program (Zukunftsinvestitionsprogramm, ZIP) of the German Federal Government is gratefully acknowledged. We thank Vladimir G. Ushakov and Anatoli I. Maergoiz for their help during the fitting procedure. We would also like to acknowledge helpful discussions with Jürgen Troe, Dirk Schwarzer, Jörg Schroeder, Klaus Luther, Jomo Walla, Sebastian Kühn and Christian Reichardt. Special thanks go to the BASF AG, and here especially Hansgeorg Ernst, for generously providing the highly purified *all-trans*-12′-apo-β-caroten-12′-al sample and extensive advice.

References

1 T. Polívka and V. Sundström, *Chem. Rev.*, 2004, **104**, 2021.
2 N. E. Holt, D. Zigmantas, L. Valkunas, X.-P. Li, K. K. Niyogi and G. R. Fleming, *Science*, 2005, **307**, 433.
3 T. W. Goodwin, *The Biochemistry of Carotenoids*, 2nd edn, Chapman & Hall, London, vol. 1, 1980.
4 S. Liaaen-Jensen, in *Carotenoids*, ed. G. Britton, S. Liaaen-Jensen and H. Pfander, Birkhäuser Verlag, Berlin, 1998, vol. 3, p. 217.
5 J. E. Johansen, W. A. Svec, S. Liaaen-Jensen and F. T. Haxo, *Phytochemistry*, 1974, **13**, 2261.
6 H. A. Frank, J. A. Bautista, J. Josue, Z. Pendon, R. G. Hiller, F. P. Sharples, D. Gosztola and M. R. Wasielewski, *J. Phys. Chem. B*, 2000, **104**, 4569.

7 R. G. Hiller, in *The Photochemistry of Carotenoids*, ed. H. A. Frank, A. J. Young, G. Britton and R. J. Cogdell, Kluwer, Dordrecht, 1999, p. 81.
8 R. P. Ilagan, R. L. Christensen, T. W. Chapp, G. N. Gibson, T. Pascher, T. Polívka and H. A. Frank, *J. Phys. Chem. A*, 2005, **109**, 3120.
9 M. Kopczynski, T. Lenzer, K. Oum, J. Seehusen, M. T. Seidel and V. G. Ushakov, *Phys. Chem. Chem. Phys.*, 2005, **7**, 2793.
10 J. A. Bautista, R. E. Connors, B. B. Raju, R. G. Hiller, F. P. Sharples, D. Gosztola, M. R. Wasielewski and H. A. Frank, *J. Phys. Chem. A*, 1999, **103**, 8751.
11 D. Zigmantas, R. G. Hiller, F. P. Sharples, H. A. Frank, V. Sundström and T. Polívka, *Phys. Chem. Chem. Phys.*, 2004, **6**, 3009.
12 D. Zigmantas, R. G. Hiller, A. Yartsev, V. Sundström and T. Polívka, *J. Phys. Chem. B*, 2003, **107**, 5339.
13 T. Lenzer, K. Oum, J. Seehusen and M. T. Seidel, *J. Phys. Chem. A*, 2006, **110**, 3159.
14 Z. He, D. Gosztola, Y. Deng, G. Gao, M. R. Wasielewski and L. D. Kispert, *J. Phys. Chem. B*, 2000, **104**, 6668.
15 J. Piel, M. Beutter and E. Riedle, *Opt. Lett.*, 2000, **25**, 180.
16 E. Riedle, M. Beutter, S. Lochbrunner, J. Piel, S. Schenkl, S. Spörlein and W. Zinth, *Appl. Phys. B*, 2000, **71**, 457.
17 T. Wilhelm, J. Piel and E. Riedle, *Opt. Lett.*, 1997, **22**, 1494.
18 S. Shima, R. P. Ilagan, N. Gillespie, B. J. Sommer, R. G. Hiller, F. P. Sharples, H. A. Frank and R. R. Birge, *J. Phys. Chem. A*, 2003, **107**, 8052.
19 C. F. Chapman and M. Maroncelli, *J. Phys. Chem.*, 1991, **95**, 9095.
20 R. Argaman and D. Huppert, *J. Phys. Chem. B*, 2000, **104**, 1338.
21 F. L. de Weerd, I. H. M. van Stokkum and R. van Grondelle, *Chem. Phys. Lett.*, 2002, **354**, 38.
22 H. H. Billsten, D. Zigmantas, V. Sundström and T. Polívka, *Chem. Phys. Lett.*, 2002, **355**, 465.
23 H. H. Billsten, J. Pan, S. Sinha, T. Pascher, V. Sundström and T. Polívka, *J. Phys. Chem. A*, 2005, **109**, 6852.
24 ORIGIN 7.5E, OriginLab Corp., Northampton, MA 01060, USA, 2004.
25 E. Lippert, *Z. Naturforsch., A*, 1955, **10**, 541.
26 N. Mataga, Y. Kaifu and M. Koizumi, *Bull. Chem. Soc. Jpn.*, 1956, **29**, 465.
27 B. Valeur, *Molecular Fluorescence—Principles and Applications*, Wiley-VCH, Weinheim, 2002.
28 *Handbook of Chemistry and Physics*, 85th edn, CRC Press, Boca Raton, 2004.
29 D. Zigmantas, T. Polívka, R. G. Hiller, A. Yartsev and V. Sundström, *J. Phys. Chem. A*, 2001, **105**, 10296.
30 D. A. Wild, K. Winkler, S. Stalke, K. Oum and T. Lenzer, to be published.
31 H. A. Frank, V. Chynwat, R. Z. B. Desamero, R. Farhoosh, J. Erickson and J. Bautista, *Pure Appl. Chem.*, 1997, **69**, 2117.
32 V. Chynwat and H. A. Frank, *Chem. Phys.*, 1995, **194**, 237.
33 R. Englman and J. Jortner, *Mol. Phys.*, 1970, **18**, 145.